ARTICLES
https://doi.org/10.1038/s41477-018-0253-3
nature plants

Molecular basis of flowering under natural long-day conditions in *Arabidopsis*

Young Hun Song[1,2,8*], Akane Kubota[1,8], Michael S. Kwon[1], Michael F. Covington[3], Nayoung Lee[1], Ella R. Taagen[1], Dianne Laboy Cintrón[1], Dae Yeon Hwang[2], Reiko Akiyama[4], Sarah K. Hodge[5], He Huang[6], Nhu H. Nguyen[1], Dmitri A. Nusinow[6], Andrew J. Millar[5], Kentaro K. Shimizu[4,7] and Takato Imaizumi[1*]

Plants sense light and temperature changes to regulate flowering time. Here, we show that expression of the Arabidopsis florigen gene, FLOWERING LOCUS T (FT), peaks in the morning during spring, a different pattern than we observe in the laboratory. Providing our laboratory growth conditions with a red/far-red light ratio similar to open-field conditions and daily temperature oscillation is sufficient to mimic the FT expression and flowering time in natural long days. Under the adjusted growth conditions, key light signalling components, such as phytochrome A and EARLY FLOWERING 3, play important roles in morning FT expression. These conditions stabilize CONSTANS protein, a major FT activator, in the morning, which is probably a critical mechanism for photoperiodic flowering in nature. Refining the parameters of our standard growth conditions to more precisely mimic plant responses in nature can provide a powerful method for improving our understanding of seasonal response.

Many plants utilize day-length (that is, photoperiod) and temperature information to control various seasonal responses for survival and reproduction. Among the seasonal responses, flowering regulation in *Arabidopsis* is the most characterized response at the molecular level[1]. Photoperiod and temperature information is processed through circadian clock-dependent mechanisms to induce the expression of the florigen gene, *FLOWERING LOCUS T* (*FT*), around dusk in long days (LDs)[2,3]. This LD-specific *FT* induction occurs in leaf phloem companion cells. Once synthesized in LD, the FT protein is transferred from the leaves to the shoot apical meristem to trigger the transition from vegetative to reproductive development[4].

Many components in the *Arabidopsis* photoperiodic pathway are highly conserved in angiosperms (including major crops such as rice, wheat, barley and potato) to regulate seasonal responses. For instance, genes identified through quantitative trait locus analyses on flowering time, yield or other domestication traits (often tied with the loss or reduction of photoperiod sensitivity) in many crops frequently turned out to be homologues of the *Arabidopsis* photoperiodic flowering components[5]. The photoperiodic-sensing mechanism originally characterized in *Arabidopsis* was found to already exist in bryophytes to regulate photoperiodic reproductive development[6]. This indicates that incorporating photoperiodic information into developmental regulation has been important for land plant survival.

Thus far, *Arabidopsis* research has been instrumental in not only identifying the components involved in photoperiodic flowering but also understanding how these components function in this pathway under well-controlled laboratory settings. However, it remains unknown whether the current model of photoperiodic flowering regulation can recapitulate the seasonal flowering mechanisms in complicated natural LD environments. Here, we show the presence of a previously uncharacterized regulation of florigen induction in *Arabidopsis* plants grown in natural LD conditions and our subsequent attempt to elucidate its regulatory mechanism using laboratory growth conditions optimized to plant responses in nature.

Results

Flowering regulation under natural LD conditions. Light (day length and light quality) and temperature are major environmental parameters that control flowering time[2,3,7]. The day length and temperature conditions of the summer solstice in Seattle, WA, USA, (47° 36′ N; day length: 15 h 59 min; average high temperature from 1971 to 2000: 21.1 °C) were similar to our laboratory LD conditions (16 h, constant 22 °C). In addition, ecological studies showed that summer annuals of wild *Arabidopsis* plants grown in similar latitudes to Seattle germinate and flower within a roughly 1-month period between March and July in both Europe and North America[8–15]. Thus, we tested how accurately the photoperiodic flowering regulation that occurs in controlled laboratory environments can represent flowering regulation under similar natural LD conditions.

We grew wild-type (WT; Columbia-0 (Col-0)) plants outside in Seattle in June and harvested them around the summer solstice (Fig. 1a and Supplementary Fig. 1). We analysed the expression of genes important for photoperiodic flowering regulation[3] (Fig. 1b,c and Supplementary Fig. 2). The expression patterns of six circadian clock genes, clock output flowering genes and floral repressor genes were relatively similar to those already described in the laboratory-grown samples[16–19] (Supplementary Fig. 2). In addition, the night-peaking *CONSTANS* (*CO*) expression profile was similar to the one in the laboratory LD condition with cooler nights[19] (Fig. 1b). These results indicate that simplified laboratory conditions recapitulate

[1]Department of Biology, University of Washington, Seattle, WA, USA. [2]Department of Life Sciences, Ajou University, Suwon, Korea. [3]Amaryllis Nucleics, Oakland, CA, USA. [4]Department of Evolutionary Biology and Environmental Studies, University of Zurich, Zürich, Switzerland. [5]School of Biological Sciences and SynthSys, University of Edinburgh, Edinburgh, UK. [6]Donald Danforth Plant Science Center, St. Louis, MO, USA. [7]Kihara Institute for Biological Research, Yokohama City University, Yokohama, Japan. [8]These authors contributed equally: Young Hun Song, Akane Kubota.
*e-mail: younghsong@ajou.ac.kr; takato@uw.edu

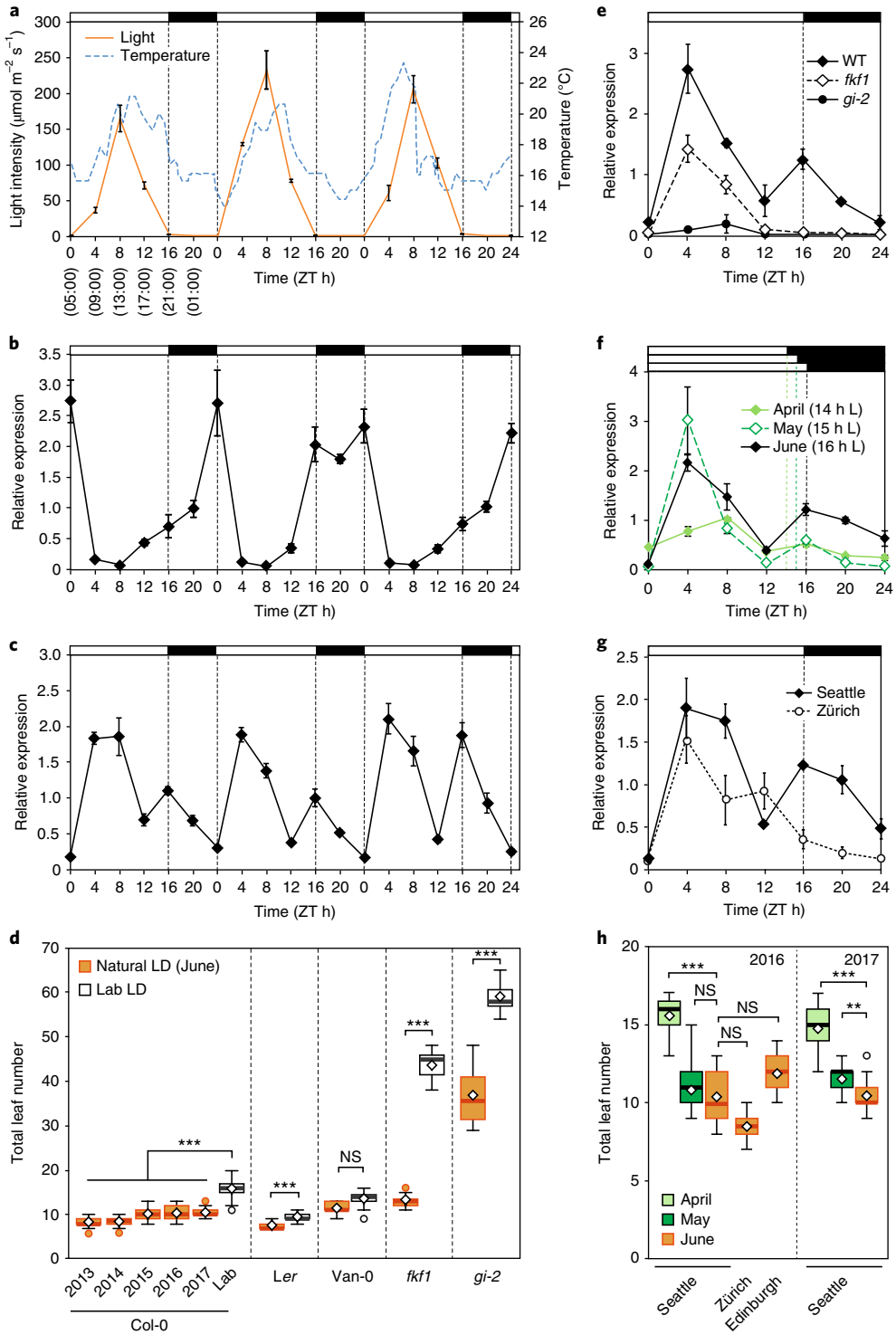

Fig. 1 | The florigen *FT* gene is induced in the morning in natural LD conditions. a, Changes in light intensity and temperature on the days near the summer solstice in 2013 when the samples were harvested. For outside conditions, ZT0 was set as the sunrise time (that is, 05:00 in Seattle from 23 June 2013 to 25 June 2013). Light intensity results are the means ± s.e.m. from different growth areas ($n = 3$). Temperature data were obtained from a nearby weather station. **b**,**c**, Expression profiles of *CO* (**b**) and *FT* (**c**) under the conditions shown in **a**. All gene expression results (means ± s.e.m.) in this paper were normalized against *IPP2* and *PP2A* ($n = 3$ biologically independent samples). **d**, Flowering time results of plants grown outside in June and in laboratory LD conditions. Each box is located between the upper and the lower quartiles and the whiskers indicate the 1.5-times interquartile ranges. The thick horizontal lines in the boxes represent the median and the open diamonds represent the mean. Outliers are indicated by circles. $12 \leq n \leq 100$, $^{***}P < 0.001$, NS, not significant; linear models or generalized linear models were used throughout the paper (for details on statistical information, see Supplementary Table 3). **e**, *FT* expression profiles in WT plants, *fkf1* and *gi-2* mutants grown outside around the summer solstice in 2017. **f**, *FT* expression profiles in WT plants grown at different times in spring in 2016. The day length (hours (h) in light (L)) on the day of harvesting is indicated for each month. **g**, *FT* expression profiles in WT plants grown around the summer solstice in Seattle and Zürich in 2016. For **e**–**g**, $n = 3$ biologically independent samples, and the results represent the means ± s.e.m. **h**, Flowering phenotypes of WT plants grown in different months and locations in spring. The details of the box plots are the same as those in **d** ($n \geq 11$, $^{**}P < 0.01$, $^{***}P < 0.001$, NS, not significant (for details on statistical information, see Supplementary Table 3)).

the natural gene expression profiles of those genes. However, in the plants grown outside, *FT* showed a bimodal expression pattern with peaks in the morning and around dusk (Fig. 1c), which clearly differed from the typical *FT* pattern peaking near dusk in the laboratory LD conditions[17,20]. We also observed a similar bimodal expression pattern in *TWIN SISTER OF FT* (*TSF*), a related florigen gene[20] (Supplementary Fig. 2l).

As *FT* levels strongly correlate with flowering time[19,21], we analysed the flowering time of Col-0 plants grown in natural LD conditions. During the past 5 years, even though temperatures around the summer solstice varied (Supplementary Fig. 1), Col-0 plants all flowered at similar developmental times with fewer leaves than plants grown in laboratory LD conditions (Fig. 1d). In addition, we repeatedly observed similar *CO* and *FT* expression patterns in samples harvested around the summer solstices from 2013 to 2017 (Fig. 1b,c,e–g and Supplementary Figs. 3 and 5). We also grew other accessions, such as a common laboratory accession, Landsberg *erecta* (L*er*), and another WT accession, Vancouver-0 (Van-0; isolated from Vancouver, BC, Canada; 49° 15′ N) in natural LD conditions. We speculated that Van-0 is adapted to an environment similar to Seattle. Both accessions flowered earlier than Col-0 plants in laboratory LD conditions, even slightly earlier in natural LD conditions (Fig. 1d), and showed bimodal *FT* expression patterns in natural LD conditions (Supplementary Fig. 4).

We also analysed the phenotypes of some non-transgenic alleles of photoperiodic flowering mutants, such as *flavin-binding, kelch repeat, f-box 1* (*fkf1*) and *gigantea* (*gi-2*), in natural LD conditions. The flowering time of these late-flowering mutants was significantly earlier than that in laboratory LD conditions (Fig. 1d). The *fkf1* mutant flowered at almost the same time as Col-0 plants in natural LD conditions, suggesting that some regulation that takes place outside but not in the laboratory may trigger earlier flowering in the *fkf1* mutant. When we analysed *FT* expression patterns in *fkf1* and *gi-2* grown in natural LD conditions, the *gi-2* mutant lost *FT* expression as expected[22], but the morning *FT* expression was clearly observed in the *fkf1* mutant (Fig. 1e). These results suggest that morning *FT* expression in the *fkf1* mutant is probably the cause of the early flowering phenotype of *fkf1* in natural LD conditions.

As our results suggested a functional contribution of morning *FT* expression on flowering in natural LD conditions, we analysed the expression patterns of *FT* in samples grown in different times in spring (April, May and June), which is the growth season of summer annuals[8–12,14]. In Seattle, the days are already lengthening in April (approximately 14 h); however, the ambient temperature in April was colder than in May and June (Supplementary Fig. 1). Col-0 plants flowered later in April than in May and June (Fig. 1h). In all samples grown during spring in 2016 and 2017, *FT* expression peaked in the morning with different levels (lower in April than in May and June) without changing *CO* expression patterns (Fig. 1f and Supplementary Fig. 5).

Next, we tested whether the *FT* morning peak is observed in two native locations of *Arabidopsis*. We grew Col-0 plants in Zürich (47° 37′ N, similar latitude to Seattle) and in Edinburgh (55° 57′ N) in June. Although the temperatures (and day length in Edinburgh) were different than in Seattle (Supplementary Figs. 1 and 6), Col-0 plants grown in both locations flowered at a similar developmental timing to the ones grown in Seattle (Fig. 1h). Both samples also showed the morning expression of *FT*, although the afternoon *FT* expression levels differed (Fig. 1g and Supplementary Fig. 7c). These results indicate that WT plants grown in natural LD conditions induce *FT* expression in the morning and possibly around dusk to induce early flowering.

Reconstitution of laboratory growth conditions that reflect natural conditions for flowering. Our results obtained from plants grown in natural LD conditions demonstrated that our current laboratory LD conditions are not sufficient to reproduce all important flowering regulation. To more precisely study these mechanisms, we adjusted our current growth conditions using *FT* expression patterns as a proxy for the flowering regulation in nature. We first hypothesized that the daily light intensity changes might alter the *FT* expression pattern, compared to step changes (that is, light on/off) under laboratory conditions. The light intensity changes did not drastically alter the *FT* expression pattern (or *CO* and *TSF*) (Supplementary Fig. 8a–e), indicating that light on/off conditions might be sufficient. Daily temperature changes affect *FT* expression patterns[19,23]; thus, we analysed the effect of daily temperature fluctuation on *FT* expression. When Col-0 plants were grown in laboratory LD conditions with daily temperature oscillations based on the average changes that occurred around the summer solstice (Supplementary Fig. 8f,g), *CO* expression was strongly induced at the end of the night (Supplementary Fig. 8h). The afternoon *FT* expression levels (but not the *TSF* expression levels) were severely repressed by daily temperature changes (Supplementary Fig. 8i,j). These results suggest that temperature oscillation is not enough to induce *FT* expression in the morning, although it can repress *FT* in the afternoon.

The red/far-red (R/FR) ratio in an open field (including our outside conditions) is approximately 1 (ref. [24]), but it varies from approximately 2 (in our laboratory conditions) to 13 (ref. [24]) under fluorescent lamps. Plant shade conditions (that is, very low R/FR ratios) highly induce *FT* expression even in the morning[25,26]. We wondered whether the morning *FT* expression could be induced under R/FR ratio = 1 conditions. To test this, we supplemented our fluorescent lamps (R/FR = 2) with dim far-red LEDs to adjust the R/FR ratio to 1 (Supplementary Fig. 9a). Merely adjusting the R/FR ratio from 2 to 1 was sufficient to induce *FT* (and *TSF*) expression in the morning, without affecting *CO* expression patterns (Fig. 2a and Supplementary Fig. 9b,c). Under these conditions (named LD + FR), the levels of both morning and afternoon *FT* expression were higher than in laboratory LD conditions (Fig. 2a). However, the afternoon *FT* peak was still slightly higher than the morning peak, which is different from the *FT* expression patterns in natural LD conditions. We also tested whether R/FR = 1 induces *FT* expression in the morning independent of photoperiod changes. We analysed *FT* expression in short days (SDs) with R/FR = 1 (SD + FR). *FT* expression was not induced in SD + FR, similar to regular SD conditions (Supplementary Fig. 10), implying that the morning induction of *FT* expression under LD + FR conditions is LD specific.

As temperature oscillation reduced afternoon *FT* expression levels (Supplementary Fig. 8i), we hypothesized that combining the R/FR = 1 conditions with daily temperature changes may cause a similar *FT* expression pattern to that observed outside. Incorporating these two parameters in the simplified laboratory conditions (LD + FR + temperature (temp)) was sufficient to generate similar *FT* expression patterns (and *CO* and *TSF*) to that observed in nature (Fig. 2b and Supplementary Fig. 11). We then analysed the flowering time of WT accessions and photoperiodic mutants including *co*, *ft*, *ft tsf* and *fkf1* under the LD + FR + temp conditions. WT plants and the *fkf1* mutant alleles (*fkf1* and *fkf1-2*) flowered earlier in LD + FR + temp conditions than in laboratory LD conditions (Fig. 2c). In addition, the *FT* expression profile in *fkf1-2* plants was similar to that in *fkf1* plants grown in natural LD conditions (Supplementary Fig. 12), validating that the simplified LD + FR + temp conditions captured the major environmental parameters to recreate the *FT* expression patterns and flowering time responses of the plants grown in natural LD conditions. Importantly, the *co*, *ft* single and *ft tsf* double mutants still showed a similar late-flowering phenotype under all experimental conditions (Fig. 2c). In addition, the *ft-1 tsf-1* double mutants flowered later than the *ft-1* mutant (Fig. 2c), indicating that changes in the expression patterns of both *FT* and *TSF* may contribute to flowering time in LD + FR + temp conditions.

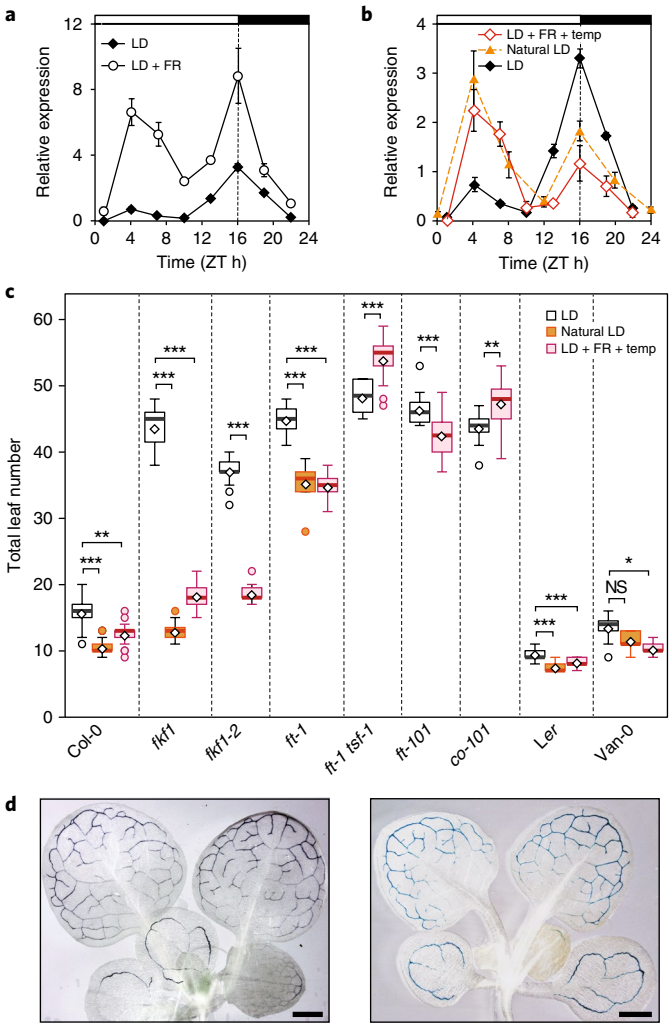

Fig. 2 | Adjusting the R/FR ratio to 1 and changing the daily temperature of the laboratory growth conditions are sufficient to recreate the *FT* profiles and flowering of plants grown in natural LD conditions. a,**b**, *FT* expression profiles in LD and LD + FR (**a**), and in LD, LD + FR + temp conditions and natural LD in 2014 (**b**). The results represent the means ± s.e.m. ($n = 3$ biologically independent samples). **c**, Flowering phenotypes of WT accessions and photoperiodic mutants in LD + FR + temp conditions. Each box is located between the upper and the lower quartiles and the whiskers indicate the 1.5-times interquartile ranges. The thick horizontal lines in the boxes represent the median and the open diamonds represent the mean. Outliers are indicated by circles. $n \geq 11$, $^{*}P < 0.05$, $^{**}P < 0.01$, $^{***}P < 0.001$, NS, not significant (for details, see the statistical information in Supplementary Table 3). **d**, Spatial expression patterns of *FT* in LD + FR + temp. *FT:GUS* plants were grown in LD + FR + temp conditions for 2 weeks and harvested at ZT4 ($n = 4$–5 independent plants, repeated twice biologically) (right panel). As a comparison, *FT:GUS* plants were grown in LD conditions and harvested at ZT4 ($n = 5$ independent plants) (left panel). The staining patterns of GUS activity in the LD-grown samples harvested in ZT4 resembled those in the ones harvested at the end of the day (ZT16) (Supplementary Fig. 13), most likely due to the very stable nature of the GUS protein[79]. Scale bars, 1 mm.

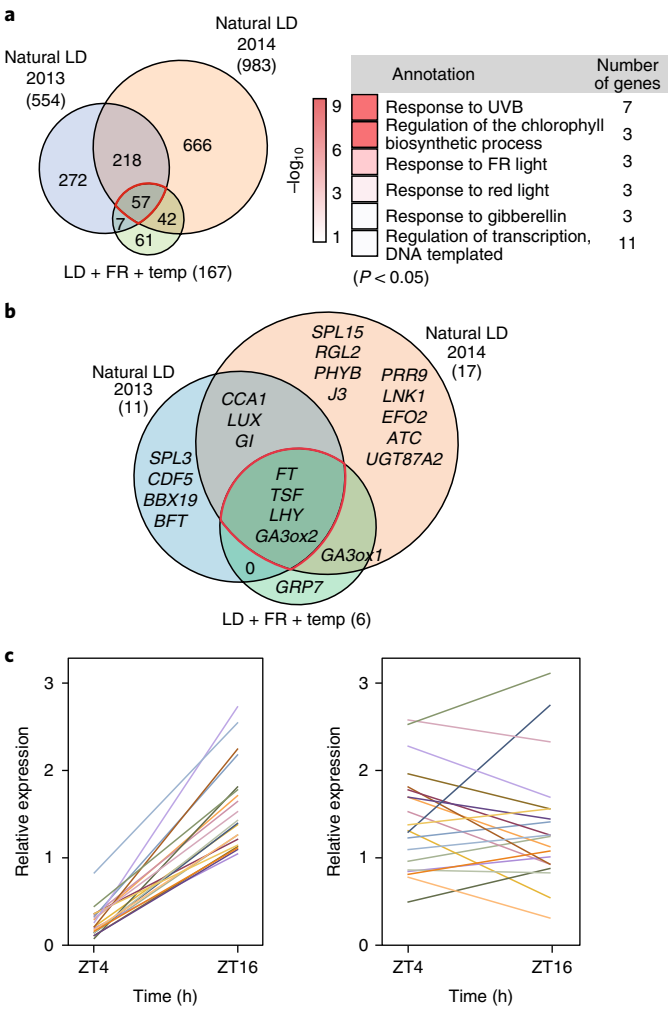

Fig. 3 | Morning induction of florigen expression occurs under both natural LD and LD + FR + temp conditions and is a common response in WT accessions. a, The upregulated genes of RNA sequencing results in 2-week-old samples harvested at ZT4 in 2013, 2014 and LD + FR + temp conditions compared with the ZT4 samples in laboratory LD conditions ($n = 3$ biologically independent samples). The Gene Ontology term categories enriched in the 57 genes are shown. The *P* values represent one-tailed Fisher exact probability values. See Supplementary Table 1 for the actual values. **b**, Flowering-related genes in FLOR-ID were extracted from the data set shown in **a**. **c**, *FT* expression levels in the morning (ZT4) and at dusk (ZT16) in 20 *Arabidopsis* WT accessions (Supplementary Fig. 15) in LD (left) and LD + FR + temp (right) conditions.

We also analysed whether the LD + FR + temp conditions changed the spatial expression patterns of *FT* to induce its morning peak. The tissue-specific GUS activity patterns in the *FT:GUS* plants were similar in LD, LD + FR and LD + FR + temp conditions (Fig. 2d and Supplementary Fig. 13), indicating that the adjustment of the R/FR ratio and temperature mainly affected the temporal expression pattern of *FT*.

To explore the similarities between LD + FR + temp and natural LD conditions on a whole-transcriptome scale, we performed RNA sequencing analysis using WT plants grown in laboratory LD, LD + FR + temp and 2 years (2013 and 2014) of natural LD conditions. The samples were harvested at Zeitgeber time 4 (ZT4; the time after light onset) when morning *FT* expression peaks. Compared with laboratory LD conditions, 57 genes were consistently upregulated in the morning in 2 different years of natural LD and LD + FR + temp conditions (Fig. 3a and Supplementary Table 1). Gene Ontology term enrichment analysis showed that genes involved in light (UVB, far-red and red) responses were enriched (Fig. 3a and Supplementary Table 1). Among these 57 genes, only 4, including *FT* and *TSF*, were identified as flowering genes, based on

Flowering Interactive Database (FLOR-ID)[27] (Fig. 3b). In the downregulated genes common among the three conditions compared with the laboratory LD condition, environmental stress-related genes were enriched (Supplementary Fig. 14a,b and Supplementary Table 1). However, there were no downregulated flowering genes overlapping among the three conditions (Supplementary Fig. 14c). These results indicate that *FT* and *TSF* induction levels might be the major difference important for flowering time regulation between LD and LD + FR + temp as well as natural LD conditions.

Flowering time is a critical adaptive trait within WT accessions[28]. Our data showed that the generation of the *FT* morning peak was closely related to the early-flowering phenotypes in natural LD conditions (Fig. 1c–h). We asked whether this mechanism is widely conserved in WT accessions. To test this, we compared *FT* expression levels between morning and evening among 20 summer annual accessions[29] originating from different latitudes (Supplementary Fig. 15a) grown in laboratory LD and LD + FR + temp conditions. In LD conditions, the *FT* expression levels in all accessions were significantly higher in the afternoon than in the morning (Fig. 3c and Supplementary Fig. 15b). However, in LD + FR + temp conditions, the differences in *FT* expression levels between the morning and the evening were much reduced (Fig. 3c and Supplementary Fig. 15c). These results suggest that the mechanisms that induce morning *FT* expression in LD + FR + temp conditions are largely conserved across *Arabidopsis* accessions.

Components important for flowering time regulation in nature. As our LD + FR + temp conditions reproduced *FT* expression profiles similar to those in natural LD conditions (Fig. 2b), we next investigated whether any known components in the flowering and light signalling pathways are involved in the regulation of morning *FT* expression. Because CO is a chief activator of *FT*[1], we first analysed *FT* expression in the *co* mutant. *FT* expression levels in the *co* mutant were very low throughout the day in LD + FR + temp, LD and LD + FR conditions (Fig. 4a–c), implying that CO function is essential for *FT* induction even under conditions that are more similar to the natural environment. We then analysed *FT* expression patterns in photoreceptor and light signalling mutants, circadian clock mutants and mutants in the ambient temperature flowering pathway in LD + FR + temp conditions[1,3,30] (Fig. 4a–f and Supplementary Fig. 16). Compared with WT plants, *FT* expression in the morning was specifically reduced in the *phytochrome A* (*phyA*) mutant (*phyA-211*) in LD + FR + temp conditions (Fig. 4a). This phenotype was also pronounced in LD + FR conditions (Fig. 4b,c). These results prompted us to analyse the flowering phenotype of the *phyA* mutant in natural LD and LD + FR + temp conditions. To grow the *phyA* mutant outside, we utilized the non-transgenic *phyA-201* allele (L*er* background), as *phyA-211* possesses a transgene[31]. The *phyA-201* mutant flowered later than L*er* plants outside (Supplementary Fig. 17a). Previous studies posited that a certain amount of FR light is required to observe phyA-dependent effects on flowering, as *phyA* mutants only showed a late-flowering phenotype in LD conditions with a lower R/FR ratio in the afternoon or in continuous FR light conditions[7,32]. In LD + FR + temp conditions, both *phyA-201* and *phyA-211* mutants flowered later than their parental accessions (Supplementary Fig. 17a). These results indicate that both natural LD and LD + FR + temp conditions (R/FR = 1) contain enough FR light to observe the phyA contribution to flowering induction. We also analysed *FT* expression in the *phyA-201* mutant and found that *FT* expression levels were lower in both the morning and the afternoon than L*er* plants (Supplementary Fig. 17b,c). This result indicates that, although phyA is clearly involved in *FT* induction in the morning, its contribution to afternoon *FT* expression may differ in either different backgrounds and/or alleles. We further assessed the significance of phyA signalling using the *far-red elongated hypocotyl 1* (*fhy1*) *fhy1-like* (*fhl*) mutant (Col-0 background) in which phyA signalling is severely attenuated due to impairment of phyA nuclear transport[33]. Although the phenotype was weaker than the *phyA-211* mutant, *fhy1 fhl* also showed a reduction in morning *FT* expression level in LD + FR + temp conditions (Supplementary Fig. 16a,b). This result further supports the notion that phyA signalling is involved in flowering regulation through inducing *FT* in natural LD conditions.

phyA functionally antagonizes phyB in flowering[34,35]. In the *phyB* mutant, *FT* expression levels were higher than in WT plants in LD + FR + temp conditions (Fig. 4d). In *early flowering 3* (*elf3*), which is a phenocopy of the *phyB* mutants[36], *FT* expression levels were even higher than in the *phyB* mutant (Fig. 4d–f). The difference between the *phyB* and *elf3* mutants was more pronounced in LD and LD + FR conditions (Fig. 4d–f). These results suggest that ELF3 may regulate not only phyB signalling but also other signalling pathways that are important for *FT* induction.

Despite being downstream signalling components of phyB and ELF3 (refs [37,38]), PHYTOCHROME INTERACTING FACTOR 1 (PIF1), PIF3, PIF4 and PIF5 might not be important for *FT* induction in LD + FR + temp conditions, as *FT* expression profiles in the *pif1 pif3 pif4 pif5* (*pifq*) mutant resembled that in WT plants (Supplementary Fig. 16c,d). The *FT* expression levels in both *constitutive photomorphogenic 1* (*cop1*) and the *suppressor of phyA-105 1* (*spa1*) *spa3 spa4* triple mutants were higher than in WT plants without changing *CO* mRNA patterns (Supplementary Fig. 16c,d). As COP1 and SPAs directly control CO protein degradation[39,40], this indicates that CO protein stability regulation is still important in LD + FR + temp conditions. In the *cryptochrome 1* (*cry1*) *cry2* double mutant, *FT* expression occurred just in the morning (Supplementary Fig. 16e,f). This result prompted us to analyse the flowering phenotype in LD + FR + temp conditions. The *cry1 cry2* mutant flowered significantly earlier in LD + FR + temp conditions than in LD conditions (Supplementary Fig. 18), which resembles the flowering phenotypes of *fkf1* mutants. This result further indicates that the morning expression of *FT* contributes to flowering time regulation.

Circadian clock components often regulate *FT* expression in LD conditions[1]. *FT* expression levels were depressed in both *gi* and *pseudo response regulator7* (*prr7*) *prr9* mutants in LD + FR + temp conditions (Supplementary Fig. 16e–h). In the *circadian clock associated 1* (*cca1*) *late elongated hypocotyl* (*lhy*) double mutant, *FT* expression levels during the afternoon were strongly increased in LD + FR + temp conditions (Supplementary Fig. 16g,h). Based on these mutant phenotypes, our results suggest that *GI* and *PRR* genes are important for the induction of *FT* throughout the day[22,41], whereas the morning clock genes, *CCA1* and *LHY*, strongly repress *FT* mainly in the afternoon[1,42].

In the ambient temperature pathway mutants, such as *short vegetative phase* (*svp*), the triple mutant of *svp flowering locus m* (*flm*) *flowering locus c* (*flc*), and *high expression of osmotically responsive genes 1* (*hos1*)[29,43], the difference in morning *FT* expression levels looked greater than that in the afternoon (Supplementary Fig. 16i,j). This could be due to lower temperatures in the morning, which activate the ambient temperature pathway. In summary, based on our results, several known components are involved in morning *FT* expression regulation.

To further investigate the mechanisms of morning *FT* induction, we studied possible interactions between phyA and ELF3. Our results showed that phyA functions as an *FT* activator, whereas ELF3 is a *FT* repressor in the morning in LD + FR + temp conditions (Fig. 4a,d). In addition, phyA was identified as one of the proteins co-immunoprecipitated with ELF3, indicating that phyA and ELF3 may exist in the same protein complex[44]. First, as *FT* expression levels are highly increased under lower R/FR ratios, *FT* expression levels are the major determinants of plant-shade-induced flowering timing[25,26,45] and because the R/FR = 1 condition is enough to

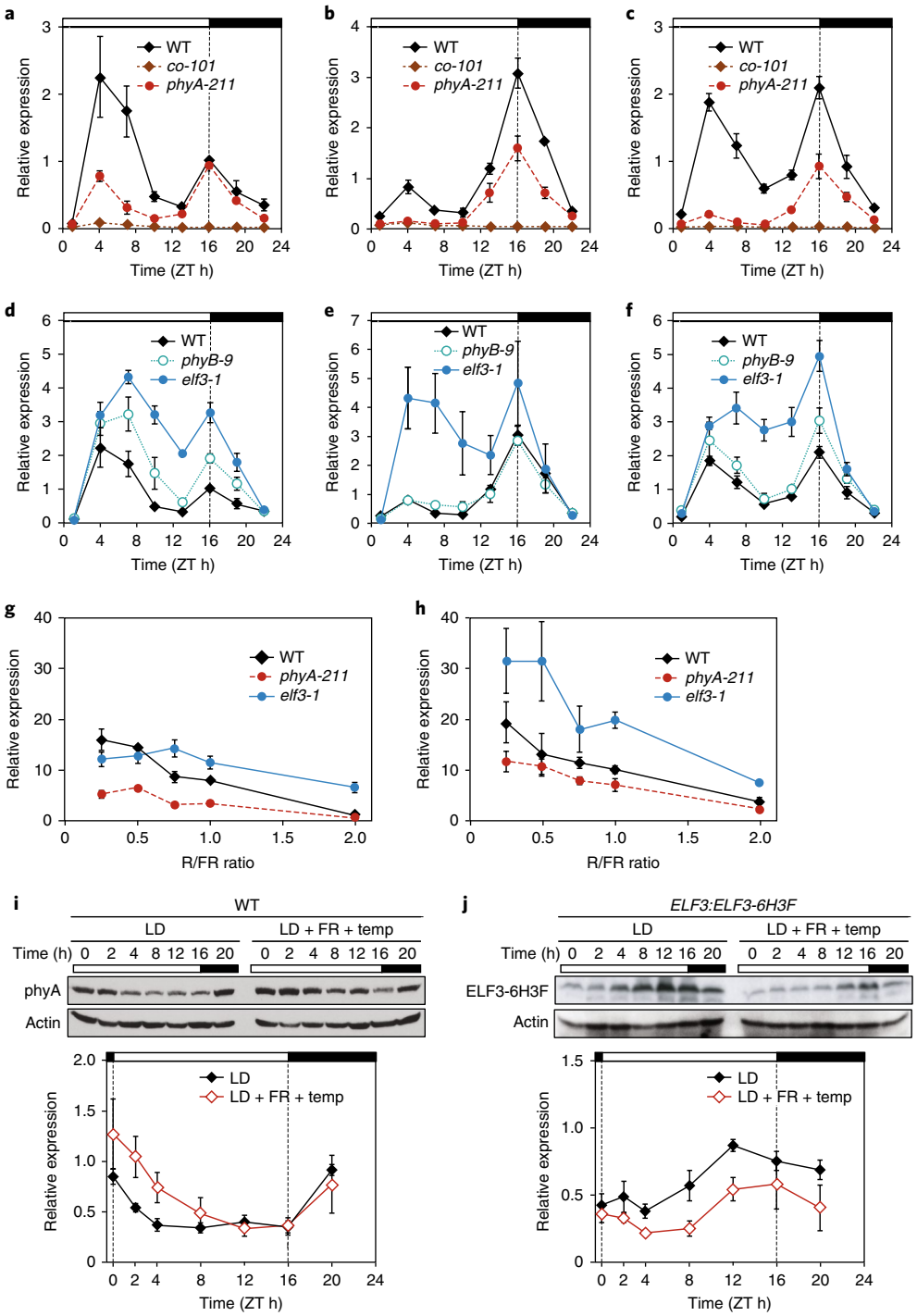

Fig. 4 | phyA and ELF3 are involved in the regulation of morning *FT* expression in LD + FR + temp conditions. a–**c**, *FT* expression profiles in WT plants, *co-101* and *phyA-211* mutants in LD + FR + temp (**a**), LD (**b**) and LD + FR (**c**) conditions. **d**–**f**, *FT* expression profiles in WT plants, *phyB-9* and *elf3-1* mutants in LD + FR + temp (**d**), LD (**e**) and LD + FR (**f**) conditions. **g**,**h**, *FT* expression levels in WT plants, *phyA-211* and *elf3-1* mutants in LD conditions with different R/FR ratios. The expression levels of *FT* in these plants in the morning, ZT4 (**g**), and at dusk, ZT16 (**h**), are shown. For **a**–**h**, the results represent the means ± s.e.m. ($n = 3$ biologically independent samples). **i**, Daily accumulation patterns of the phyA protein in LD and LD + FR + temp conditions. **j**, Daily accumulation patterns of the ELF3 protein in *ELF3:ELF3-6H3F* plants in LD and LD + FR + temp conditions. For both **i** and **j**, the representative blot images are shown. Actin was used as a loading control. The protein quantification results (the relative values against the loading control) represent the means ± s.e.m. ($n = 6$ biologically independent samples).

induce *FT* in the morning, we investigated the more comprehensive relationship between R/FR ratios and *FT* expression levels. We also analysed whether the *phyA* and *elf3* mutations affect *FT* expression levels in LD conditions with different R/FR ratios. In WT plants, there is nearly a linear relationship between the decrease in the R/FR ratios and the increase in *FT* expression levels in the morning (ZT4) and in the afternoon (ZT16) (Fig. 4g,h). In the *phyA-211* mutant, morning *FT* induction was severely reduced under a wide range of R/FR ratios, whereas morning *FT* expression levels in the *elf3-1* mutant were constantly high (Fig. 4g). In both *phyA-211* and

elf3-1 mutants, the *FT* expression levels over different R/FR ratios stayed at nearly similar levels at ZT4 (Fig. 4g), indicating that the function of both proteins is required to tune *FT* expression levels in response to R/FR ratio changes during the morning. In the afternoon, the lack of *elf3* made the plants more sensitive to the R/FR ratio changes, with a large increase in *FT* expression levels under lower R/FR ratios (Fig. 4h). There was only a small *phyA-211* mutation effect on afternoon *FT* expression levels (Fig. 4h). These results suggest that both phyA and ELF3 have time-dependent functions in light-quality-controlled *FT* level regulation.

We next studied the genetic relationship between *PHYA* and *ELF3* in this regulation. There was an intermediate level of *FT* expression in the *phyA-211 elf3-1* double mutant compared to *FT* expression levels in each mutant under all conditions (Supplementary Fig. 19), indicating that phyA and ELF3 function antagonistically on *FT* regulation. As a biochemical study indicated the presence of a phyA–ELF3 complex[44], we examined whether our modified LD conditions influence the amount of phyA co-immunoprecipitated with the ELF3 protein. In LD conditions, the phyA protein dissociated from the ELF3 complex as soon as the light was turned on, whereas in both LD + FR and LD + FR + temp conditions, similar amounts of phyA were co-immunoprecipitated with ELF3 at later time points during the morning (Supplementary Fig. 20). These results suggest that the prolonged presence of the phyA–ELF3 complex in LD + FR + temp conditions may change the expression levels and/or activity of phyA and/or ELF3 proteins.

We also analysed the phyA and ELF3 protein expression patterns in LD + FR + temp conditions. The accumulation levels of the phyA protein in LD + FR + temp conditions were higher during the morning than in LD conditions, although they eventually reached trough level by the end of the day (Fig. 4i). This is probably controlled by post-translational regulation, as *PHYA* transcript levels under these conditions were very similar (Supplementary Fig. 21a). By contrast, the ELF3 protein levels in LD + FR + temp conditions were lower throughout the day than in LD conditions (Fig. 4j). The *ELF3* transcript levels in LD + FR + temp conditions were also slightly lower than in LD conditions (Supplementary Fig. 21b). A higher expression of *FT* at ZT4 in LD + FR + temp conditions is consistent with the higher level of its activator phyA and lower levels of its repressor ELF3 under these conditions.

We further analysed whether ELF3 affects phyA protein patterns or vice versa. In LD + FR + temp conditions, there was no difference in *PHYA* expression levels between WT plants and the *elf3* mutant (Supplementary Fig. 22a). The phyA protein levels were slightly higher in *elf3* mutants than in WT plants, although the difference was not significant (Supplementary Fig. 22c). There were reduced levels of the ELF3 protein in *phyA* mutants than in WT plants without affecting transcript levels (Supplementary Fig. 22b,d), suggesting that phyA may regulate ELF3 protein levels post-transcriptionally in LD + FR + temp conditions. However, as ELF3 is a repressor of *FT*, the reduction of ELF3 levels in the *phyA* mutants cannot be the major cause of the reduction of *FT* expression levels in *phyA* mutants. Previous work showed that ELF3 forms a complex with a large number of light signalling and circadian clock components, many of which require functional phyB to physically associate with the ELF3 complex[44]. In addition, increased levels of phyA protein were co-immunoprecipitated with ELF3 after dawn in LD + FR + temp conditions (Supplementary Fig. 20). Thus, we hypothesized that phyA may affect ELF3 function by directly modulating the interaction of ELF3 with other factors in a light-dependent or temperature-dependent manner.

To assess whether phyA influences the composition of the ELF3 complex, we harvested *ELF3:ELF3-6H3F* samples with or without the *phyA* mutation in the morning of LD + FR + temp conditions and identified peptides co-immunoprecipitated with ELF3 using mass spectrometry analysis. We included *ELF3:ELF3-6H3F/phyB* as a reference. When we compared our peptide list of *ELF3:ELF3-6H3F* samples with the previous samples harvested in the afternoon[44], we noticed that our list did not contain peptides from ELF3-associated circadian clock proteins (Supplementary Table 2), suggesting that ELF3 does not assemble with the same evening complex in the morning. We identified peptides derived from COP1 but not SPA1. phyB is still important for ELF3 complex formation in the morning. The loss of *phyA* did not seem to drastically change the composition of the ELF3 complex, although fewer peptides from COP1 and phyE were detected in the *phyA* background (Supplementary Table 2). These results indicate that phyA may affect the interaction of a small number of components in the ELF3 complex. However, these results are not sufficient to evaluate whether those changes may affect either ELF3 function or *FT* transcription in the *phyA* mutant in LD + FR + temp conditions. Further analysis is required to elucidate the exact mechanism by which phyA and ELF3 antagonistically regulate *FT* expression levels in LD + FR + temp conditions.

As *CO* is required for the *FT* morning peak (Fig. 4a) and the *cop1* and *spa* triple mutants showed increased *FT* expression levels in LD + FR + temp conditions (Supplementary Fig. 16c,d), we hypothesized that CO protein levels may increase under these conditions. To test this, we analysed the diurnal expression profile of the CO protein in *CO:HA-CO* plants[46] in LD and LD + FR + temp conditions. The overall accumulation patterns of the CO protein in LD and LD + FR + temp conditions were similar (Fig. 5a). However, the CO protein levels increased more in LD + FR + temp conditions than in LD conditions at the ZT4 time point, when the *FT* morning peak was induced (Fig. 5a). Thus, we analysed a fine-scale time course of CO profiles during the morning. In LD conditions, the CO protein acutely accumulated just after dawn (ZT0.5–ZT1) but quickly degraded by ZT2 (Fig. 5b). In LD + FR + temp conditions, CO protein levels kept increasing until ZT1 and then decreased more gradually during the morning. The levels of CO protein expressed in the morning under LD + FR + temp conditions were similar to the levels around dusk (Fig. 5a,b), suggesting that the elevation of CO protein levels in LD + FR + temp conditions might contribute to morning *FT* peak generation.

CO protein levels are controlled by several E3 ubiquitin ligases, such as the COP1–SPA complex[39,40]. Both phyA and ELF3 physically interact with the COP1–SPA1 complex to regulate its function[44,47,48]. Thus, we investigated whether phyA and/or ELF3 mediate *FT* regulation through regulation of CO protein stability. We found that ELF3 is in the same CO protein complex in planta and in vivo (Fig. 5c and Supplementary Fig. 23). In addition, *FT* expression and the early-flowering phenotype of *elf3-1* mutants were largely dependent on functional *CO*, as *FT* expression levels are very low in both *co-101* and *elf3-1 co-101* mutants, and in the *elf3-1 co-101* mutant flowered just slightly earlier than the late-flowering *co-101* mutant (Supplementary Fig. 24). Although the *FT* levels in the *elf3-1 co-101* mutant are similar to those in the previously characterized *elf3-1 co-1* mutant[49], the *elf3-1 co-1* mutant showed an intermediate flowering phenotype between the *co-1* and *elf3-1* mutants[49]. This flowering time difference might be caused by the difference in the genetic backgrounds (*elf3-1 co-1* in F3 segregants between Col-0 and L*er*[49] cross versus *elf3-1 co-101* in Col-0) and/or *co* alleles. We next analysed whether ELF3 influences CO stability and found that the CO protein was more abundant in the *elf3* mutant, including at ZT4 (Fig. 5d and Supplementary Fig. 25). Together with our results that showed lower levels of the ELF3 protein in LD + FR + temp conditions, these results indicate that ELF3 may negatively influence CO stability in the morning and that LD + FR + temp conditions in part reduce the amount of the negative regulator to increase CO protein stability, consistent with increased expression of its target *FT*.

Discussion

Our results indicate that the difference in R/FR ratios and daily temperature are the main causes of the difference in flowering time

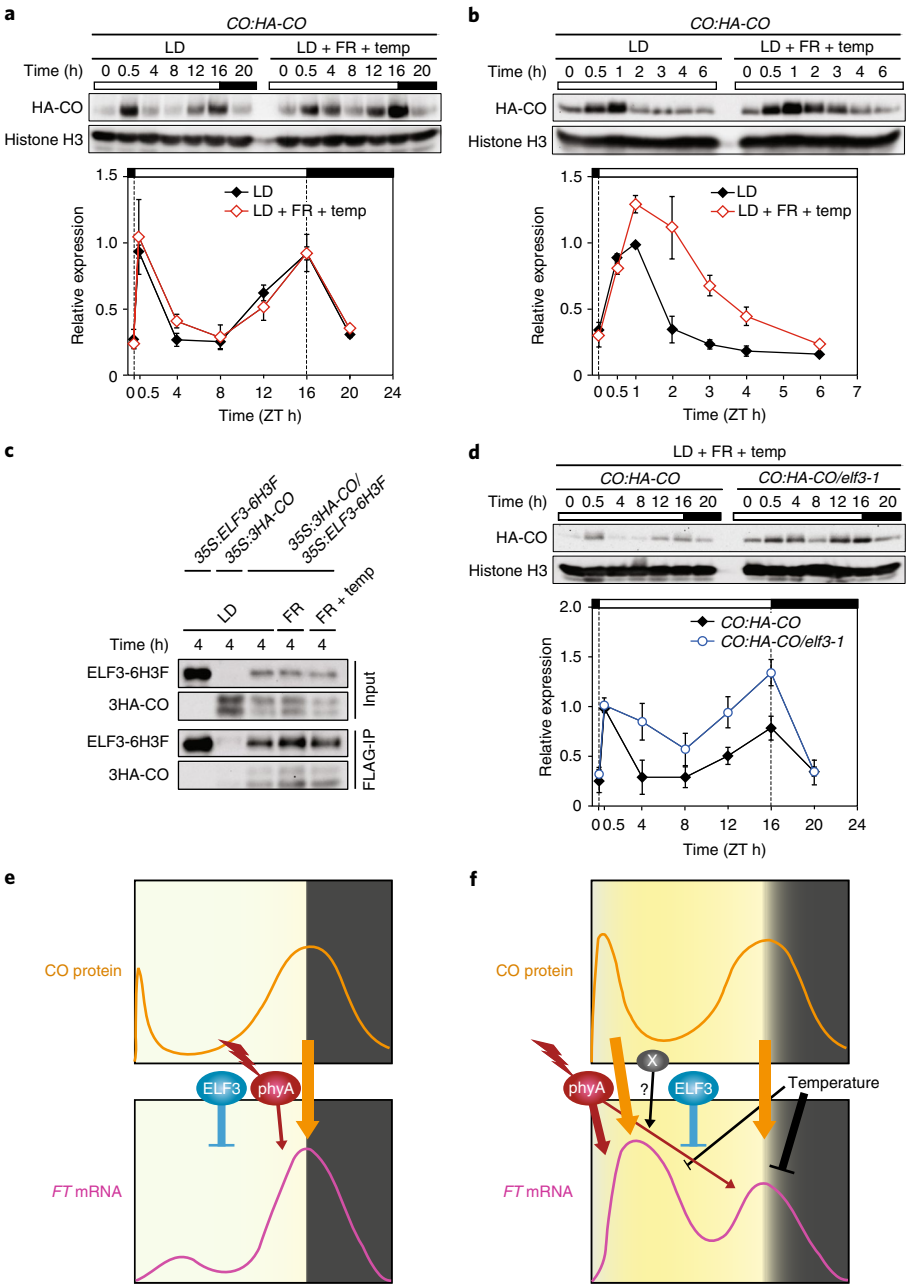

Fig. 5 | CO protein stability was increased under LD + FR + temp conditions during the morning. a,**b**, CO protein accumulation patterns in *CO:HA-CO* plants in LD and LD + FR + temp conditions. Histone H3 was used as a loading control. The quantification results represent the means ± s.e.m. ($n = 5$ (**a**) and $n = 3$ (**b**) biologically independent samples). **c**, Co-immunoprecipitation (IP) analysis of the ELF3 and CO proteins. *35S:ELF3-6H3F*, *35S:3HA-CO* and *35S:3HA-CO/35S:ELF3-6H3F* plants were grown in LD, LD + FR (labelled as FR) or LD + FR + temp (labelled as FR + temp) conditions and harvested in the morning (ZT4). The experiments were repeated three times independently and similar results were obtained. **d**, CO protein accumulation patterns in *CO:HA-CO* and *CO:HA-CO/elf3-1* plants grown in LD + FR + temp conditions. The quantification results represent the means ± s.e.m. ($n = 5$ biologically independent samples). **e**,**f**, A model for CO-dependent *FT* regulation under natural LD conditions. This model shows temporal expression patterns of the CO protein and *FT* transcripts under laboratory LD (**e**) and natural LD (**f**) conditions. In panel **e**, under artificial laboratory LD conditions in which the R/FR ratio is ≥2 and the temperature is constant, the CO protein appears to immediately accumulate after light onset and then rapidly degrade, resulting in low levels of the CO protein in the morning and early afternoon. During this period, the ELF3 protein inhibits *FT* expression through an unknown mechanism. The CO protein peaks again at the end of the day, which directly activates *FT* transcription under these conditions. In panel **f**, under natural LD conditions, the R/FR ratio is 1 and the ambient temperature oscillates throughout the day. The amount of phyA protein increases in the morning, whereas the amount of ELF3 protein decreases (Fig. 3i,j). The CO protein accumulates rapidly at high levels after sunrise and degrades more slowly under natural LD conditions than under laboratory LD conditions. This CO accumulation might be important for morning induction of *FT*. In addition to the CO protein stability changes, there might be other factors (depicted as 'X') involved in the induction of morning *FT* under natural LD conditions. The phyA signal is positively involved in *FT* induction under these conditions. ELF3 negatively acts on *FT* regulation under these conditions. In addition, the temperature oscillations strongly repress *FT* transcription in the evening. Thus, although CO protein abundance is high even at dusk, the levels of *FT* expression remain relatively low around dusk compared to the morning. We showed that we can recreate these *FT* expression profiles in the laboratory by simply adjusting the R/FR ratio of the light source and temperature conditions.

between natural LD and laboratory LD conditions. Mechanistically, this difference in growth conditions probably causes different expression levels of the florigen genes, *FT* and *TSF*, especially in the morning. Previous work indicated that *FT* induced between ZT12 and ZT20 in SD conditions was more effective for floral induction than *FT* induced during other time windows[21]. How does morning-expressed *FT* affect flowering compared to evening-expressed *FT*? The uploading of FT proteins into the phloem and the unloading of them into the shoot apical meristem are actively regulated, at least in cucurbit plants[50,51]. Phloem flux and the concentration of major transport sugars in phloem sap exhibit diurnal and developmental changes in some plants[52–54]. Thus, the efficiency of florigen movement may change depending on growth conditions, time of day and plant age. Although it is beyond the scope of our current research, it would be of interest to assess whether the timing of *FT* expression during the morning has some mechanical advantages compared to the evening in natural LD conditions.

Our results indicate that phyA and ELF3 are involved in the regulation of the morning expression of *FT* in natural LD conditions (Fig. 5e,f). In addition, the CO protein is probably more stable in the morning of natural LD conditions than in regular laboratory LD conditions. This may contribute to higher induction of *FT* in the morning. However, as the CO protein interacts with several other transcription factors to regulate *FT* in the morning[55], we assume that there are still other factors that participate in controlling *FT* expression levels in the morning in natural LD conditions (Fig. 5e,f). Thus, we think that the findings presented here are a starting point to understanding the mechanisms of the previously uncharacterized florigen induction that takes place in natural LD conditions.

With the external coincidence model for explaining photoperiodic response as a basis[56], molecular mechanisms that consist of a complex interplay between light signalling and the circadian clock have been proposed to explain LD-specific dusk *FT* expression[1]. Although our results indicate the involvement of some known flowering regulators in morning *FT* induction, the current model cannot explain how these factors induce *FT* in the morning in natural LD conditions. Investigating these mechanisms will help us to understand how *Arabidopsis* plants flower in spring in nature.

Behavioural rhythms in model animals (*Drosophila*, mouse and golden hamster) differed between natural and laboratory conditions[57–59]. In *Drosophila*, the transcriptional levels of clock genes were altered between these two conditions[60]. Even for *Arabidopsis*, previous work reported discrepancies in predicted flowering phenotypes when flowering mutants were grown outside[13], although the molecular mechanism that caused this was unknown. Based on our work, the discrepancies might be partly caused by the difference in light quality and temperature between laboratory and natural conditions. To understand the plant response at molecular levels in nature, recent functional genomic approaches in molecular ecology have successfully revealed certain mechanisms by which plants sense specific environmental stimuli in complex natural environments[61,62]. However, these approaches still have geographical and environmental limitations. Our approach for optimizing simplified laboratory conditions based on plant response in nature will be widely feasible. Studying plant responses under refined laboratory conditions that more closely reflect natural conditions will probably fill the current gap between genetics and ecology and facilitate interdisciplinary communication between them to more holistically understand the underlying mechanisms of the ever-changing phenological response in plants.

Methods

Plant materials and growth conditions. Except where indicated, all *Arabidopsis thaliana* plants—WT, *fkf1* (ref. [17]), *fkf1-2* (ref. [17]), *gi-2* (ref. [22]), *ft-1* and *ft-1 tsf-1* (ref. [63]), *ft-101* and *co-101* (ref. [64]), *phyA-211* (ref. [31]), *phyB-9* (ref. [65]), *elf3-1* (ref. [66]), *fhy1-3 fhl-1* (ref. [33]), *cop1-6* (ref. [67]), *spa1-3 spa3-1 spa4-1* (ref. [68]), *pif1 pif3 pif4 pif5* (*pifq*)[69], *cry1* (*hy4-2.23N*) *cry2-1* (ref. [70]), *cca1-1* lhy-Null* (ref. [71]), *prr7-11 prr9-10* (ref. [72]), *hos1-3* (ref. [43]), *svp-32* and *svp-32 flm-3 flc-3* (ref. [29]), *ELF3:ELF3-6H3F* and *ELF3:ELF3-6H3F/phyB-9* (ref. [44]), *CO:HA-CO* and *35S:3HA-CO*[46] and *FT:GUS*[64]—used in this study are in the Col-0 background. *phyA-201* is in the L*er* background[31]. The *ft-1* and *ft-1 tsf-1* seeds were kindly provided by M. Endo (Nara Institute of Science and Technology, Ikoma, Japan). The *fhy1-3 fhl-1* seeds were kindly provided by M. Zeidler (Justus-Liebig-University Giessen, Giessen, Germany). The *cop1-6* seeds were kindly provided by X. W. Deng (Peking University, Beijing, China). The *spa1-3 spa3-1 spa4-1* seeds were kindly provided by U. Hoecker (University of Cologne, Cologne, Germany). The *cca1-1* lhy-Null* seeds were kindly provided by R. Green (Hebrew University, Jerusalem, Israel) and S. Harmer (University of California, Davis, CA, USA). The *prr7-11 prr9-10* seeds were kindly provided by T. Yamashino (Nagoya University, Nagoya, Japan). The *svp-32* and *svp-32 flm-3 flc-3* seeds were kindly provided by J. H. Ahn (Korea University, Seoul, Korea). The WT *Arabidopsis* accessions Oy-1, RLD-1, Mh-0, An-1, Nos-0, Ma-1, Rd-0, Nd-1, En-1, Jl-3, Kz-9, Di-G, Wei-0, Ka-0, Sei-0, Mt-0 and Van-0 were all obtained from the Arabidopsis Biological Resource Center at Ohio State University (Columbus, OH, USA). The *phyA-211 elf3-1* double mutant was generated by a genetic cross between *phyA-211* and *elf3-1*. The *co-101 elf3-1* double mutant was generated by a genetic cross between *co-101* and *elf3-1*.

To generate *35S:ELF3-6H3F* transgenic lines, the pENTR/D-TOPO vector (Invitrogen) harbouring the full-length *ELF3* cDNA without a stop codon[44] was transferred to the pB7HFC binary vector[44]. The *35S:ELF3-6H3F* construct in pB7HFC was transformed into *elf3-1* plants. For *ELF3:ELF3-6H3F/phyA-211* lines, the *ELF3:ELF3-6H3F* construct in the pK7HFC vector[44] was introduced to *phyA-211* plants. To generate *35S:3HA-CO/35S:ELF3-6H3F* lines, the *35S:3HA-CO* construct in the pH7WG2 vector[46] was transformed into the *35S:ELF3-6H3F* line. The transgenic plants were selected based on the expression levels of both the *CO* and the *ELF3* genes. For *CO:HA-CO/elf3-1* lines, the *CO:HA-CO* construct in the pPZP221 binary vector[46] was transformed into *elf3-1* plants.

All plants were grown either on soil in standard flats with inserts (STF-1020-OPEN and STI-0804, T.O. Plastics; for plants grown in Seattle or similar flats/inserts for plants grown in Zürich and Edinburgh) or in sterile 1× LS agar media (Caisson) without sucrose. The soil (Sunshine Mix 4, Sun Gro Horticulture) contained a slow-release fertilizer (Osmocote 14-14-14, Scotts Miracle-Gro) and a pesticide (Bonide, Systemic Granules). After seeds were sown onto soil or growth media, they were stratified in a 4 °C room for at least 3 days and then transferred to outside growth areas or growth chambers. Only non-transgenic plants were used for the outdoor experiments, following institutional, national and international restrictions on handing genetically modified organisms (transgenic plants were only used in certified laboratory settings). For outside experiments, the flats containing stratified seeds were transferred onto a platform in a low tunnel equipped with a shading filter in our caged plant growth areas (University of Washington, University of Zürich and University of Edinburgh). To avoid shading effects from neighbouring plants, seeds were sown at a low density and, when necessary, younger seedlings were thinned to let individuals grow separately. To prevent potential light stress from excess direct sunlight exposure (which can be stronger than 1,000 μmol m^{-2} s^{-1}), the cage was covered with double layers of Reemay Garden Blanket to reduce sunlight intensity without changing the R/FR ratio. The R/FR ratio was measured by the LightScout Red/Far Red meter (Spectrum Technologies), as well as by the UV-VIS Spectrometer (StellarNet Inc). The light intensity changes around the summer solstice were measured using the LI-250A light meter (LI-COR). Temperature was directly monitored by HOBO Pendant Temperature/Light 64 K Data Loggers (Onset) for Edinburgh and Seattle. The air temperature was obtained from nearby weather station data: https://www.ed.ac.uk/geosciences/weather-station/weather-station-data for Edinburgh, http://www.meteoswiss.admin.ch/home/research-and-cooperation/nccs.html for Zurich and http://www-k12.atmos.washington.edu/k12/grayskies/nw_weather.html for Seattle, as shown in Supplementary Fig. 1. Information regarding sunrise time (ZT0) and day length in Seattle was obtained from http://aa.usno.navy.mil/data/docs/RS_OneYear.php.

Normal laboratory LD and SD conditions were described previously[46]. For FR light supplement in LD + FR and LD + FR + temp conditions, weak 730-nm FR LED light (RAY 'PfrSpec', Fluence Bioengineering, previously referred to as BML Horticulture) was provided together with full-spectrum white fluorescent light (F017/950/24, Octron Osram Sylvania) to set the R/FR = 1. To obtain dim FR light, we used a dimmer (Fluence Bioengineering/BML Horticulture) with the LED light source and also wrapped the LED light with a single layer of regular white copy paper. The R/FR ratio was adjusted using the LightScout Red/Far Red meter (Spectrum Technologies) and confirmed using the UV-VIS Spectrometer.

To apply LD + light intensity conditions, light intensity changes during the daytime shown in Supplementary Fig. 8a were set based on averages of three day-long light intensity measurements shown in Fig. 1a. Specific settings in growth chambers were as follows: ZT0, 0 μmol m^{-2} s^{-1}; ZT1, 29 μmol m^{-2} s^{-1}; ZT4, 84 μmol m^{-2} s^{-1}; ZT7, 173 μmol m^{-2} s^{-1}; ZT10, 148 μmol m^{-2} s^{-1}; ZT13, 81 μmol m^{-2} s^{-1}; and ZT16, 0 μmol m^{-2} s^{-1}. The light intensity between two settings was gradually changed in a ramping mode. The light intensity changes in the chamber were confirmed using the LI-250A light sensor (LI-COR).

For temperature fluctuation settings in the LD + temp and LD + FR + temp conditions, temperature data for 7 days around the summer solstice of 2013, from 21 to 27 June, in Seattle was obtained from a website (http://www-k12.atmos.washington.edu/k12/grayskies/nw_weather.html) and averaged. Based on the average temperature data, a multistep program shown in Supplementary Fig. 8g was set in ramping mode as follows: ZT0, 15.9 °C; ZT2, 16.2 °C; ZT4, 17.9 °C; ZT5.8, 19.4 °C; ZT9, 22.2 °C; ZT10.4, 22.6 °C; ZT11, 22.8 °C; ZT12, 22.1 °C; ZT16, 19.8 °C; ZT17, 18.3 °C; ZT20, 16.6 °C; and ZT23, 15.8 °C. The temperature changes were confirmed using HOBO Pendant Temperature/Light 64 K Data Loggers (Onset).

Flowering time was measured by the number of rosette and cauline leaves on the main stem when inflorescence reached 1–5-cm high as described previously[46]. Flowering time experiments were performed with 12 individual plants at a minimum. All flowering time results in this paper are the means ± standard errors of the means (s.e.m.).

RNA preparation and gene expression analyses. For gene expression analyses, 14-day-old seedlings grown on soil (all outside-grown samples) or LS agar plates (samples grown in the incubators) were harvested every 3 h during a 24-h period and were used for RNA extraction. RNA extraction, cDNA synthesis, quantitative PCR conditions and normalization by *ISOPENTENYL PYROPHOSPHATE/DIMETHYLALLYL PYROPHOSPHATE ISOMERASE* (*IPP2*) + *SERINE/THREONINE PROTEIN PHOSPHATASE 2A* (*PP2A*) were described previously[73]. Primers and PCR conditions for *CCA1*, *LHY*, *PRR9*, *PRR7*, *PRR5*, *TOC1*, *CDF1*, *FKF1*, *GI*, *CO*, *FT*, *FLC*, *SVP*, *IPP2* and *PP2A* were previously described[18,19,73,74]. All expression results were normalized using averages of *IPP2* and *PP2A* values. The remaining primer sequences used for analysing gene expression profiles are the following: 5′-GCACAGACTGATTAAGGTTCAAAAAC-3′ and 5′- CTTCACTGGATAGCTTTTAGCAG-3′ for *ELF3*; 5′-AATCTAGAGATCAGGTTAACGC-3′ and 5′-CTTCTTCTGACACATCTTCCT-3′ for *PHYA*; and 5′-CTCGGGAATTCATCGTATTG-3′ and 5′-CCTCTGGCAGTTGAAGTAAG-3′ for *TSF*. Quantitative PCR for *CCA1*, *LHY*, *PRR9*, *PRR7*, *PRR5*, *TOC1*, *CDF1*, *GI*, *SVP* and *IPP2* was done using the following programme: 1 min at 95 °C, followed by 40–50 cycles of 10 s at 95 °C and 20 s at 60 °C. Quantitative PCR for *FKF1*, *CO*, *FT*, *TSF*, *ELF3*, *PHYA* and *PP2A* was done using the following programme: 1 min at 95 °C, followed by 40–50 cycles of 10 s at 95 °C, 15 s at annealing temperature and 15 s at 72 °C. The annealing temperature for each primer set was 55 °C for *FKF1* and *CO*, 64 °C for *FT*, 59 °C for *TSF*, 61 °C for *ELF3*, 64.3 °C for *PHYA* and 64 °C for *PP2A*.

Whole-transcriptome RNA sequencing analysis. WT plants were grown on soil under LD, LD + FR + temp and natural LD conditions and harvested at ZT4 on day 14. The '2013 outside' samples were harvested on 25 June 2013, and the '2014 outside' samples were harvested on 7 July 2014. After mRNA was purified using NEB Next Poly(A) mRNA magnetic isolation kit (New England Biolabs), RNA sequencing libraries were prepared using the YourSeq 3′-Digital Gene Expression RNAseq Library Kit (Amaryllis Nucleics). A Bioanalyzer 2100 (High Sensitivity DNA Kit, Agilent) was used for library quality control to determine average library size, and together with concentration data from a Qubit 2.0 Fluorometer (dsDNA High Sensitivity Assay Kit, Life Technologies) to determine individual library molarity and pooled library molarity. Pooled libraries were sequenced on a NextSeq 500 (High Output v2 75 cycle kit, Illumina) to yield single-read 80-bp reads.

FASTQ sequence files were preprocessed in two steps. A Python library (clipper.py; https://github.com/mfcovington/clipper) was used to trim off the first eight nucleotides of each read to remove potential mismatches to the reference sequence caused by annealing of a random hexamer required for library synthesis. Trimmomatic v0.36 (http://www.usadellab.org/cms/?page=trimmomatic) was used to remove adapter sequences and trim or filter reads based on quality. The parameters used for Trimmomatic were 'ILLUMINACLIP:TruSeq3-PE-2.fa:2:30:10 LEADING:3 TRAILING:3 SLIDINGWINDOW:4:15 MINLEN:50'.

Preprocessed reads were mapped to the *A. thaliana* TAIR10 cDNA reference sequence (ftp://ftp.ensemblgenomes.org/pub/plants/release-34/fasta/arabidopsis_thaliana/cdna/Arabidopsis_thaliana.TAIR10.cdna.all.fa.gz) using bowtie2 with the '--norc' parameter to enforce strand-specific alignment. Read counts for each transcript in the cDNA reference were calculated using a Perl script (simple_counts.pl; https://github.com/mfcovington/read_counter).

The R package edgeR[75] was used to identify differentially expressed transcripts between samples grown in laboratory LD conditions and samples grown in LD + FR + temp conditions, outdoor samples from 2013 and 2014. Transcripts were retained for analysis if they had more than two counts per million in at least three samples. After normalization factors were calculated and dispersion estimated, pairwise comparisons were performed using the exact test in edgeR. Differentially expressed genes were then filtered using a false discovery rate cut-off of 0.05 and a minimum $\log_2$ fold change of 1. False discovery rates were calculated by adjusting *P* values for multiple comparisons using the Benjamini–Hochberg procedure[76].

Differential gene expression results were annotated using TAIR10 gene and transcript descriptions (https://www.arabidopsis.org/download_files/Genes/TAIR10_genome_release/gene_description_20131231.txt.gz). Gene ontology analysis was performed using DAVID[77].

GUS staining. For histochemical staining of GUS activity for tissue-specific expression of the *FT* gene, 14-day-old *FT:GUS* plants grown under LD, LD + FR and LD + FR + temp conditions were harvested either at ZT4 (LD + FR-grown and LD + FR + temp-grown samples) or at both ZT4 and ZT16 (LD-grown samples), and immediately treated with 90% pre-chilled acetone on ice for 10–15 min to fix and extract chlorophylls. After washing three times with 100 mM sodium-phosphate pH 7.0, whole plant tissues were submerged in the staining solution (100 mM sodium-phosphate pH 7.0, 10 mM EDTA, 0.5 mM potassium ferricyanide, 0.5 mM potassium ferrocyanide, 0.1% Triton X-100 and 1 mM X-Gluc). After 4 h of staining, the tissues were washed and dehydrated with ethanol series 30%, 50%, 80% and 100%.

Tandem affinity purification coupled mass spectrometry analysis. Fourteen-day-old *ELF3:ELF3-6H3F*, *ELF3:ELF3-6H3F/phyA-211* and *ELF3:ELF3-6H3F/phyB-9* lines grown on LS agar plates under the LD + FR + temp conditions were harvested at ZT4. Procedures for tandem FLAG and histidine immunoprecipitations, protein digestion and liquid chromatography–tandem mass spectrometry were performed according to Huang et al.[44].

Statistical analysis. Statistical analyses for flowering time experiments were done using R Statistical Computing software (v3.2.3; R Core Team). The effect of conditions on flowering time was tested using linear models when the assumptions were met in 'gvlma' function in the 'gvlma' package. When the assumptions were not met, generalized linear models with poisson error distribution (faily = poisson) were used. For more than two groups, pairwise comparisons were conducted with Tukey's multiple comparisons adjustment using 'glht' function in the 'multcomp' package.

Immunoblot analysis and protein quantification. For analysing diurnal expression profiles of the phyA, ELF3 and CO proteins, 14-day-old *Arabidopsis* seedlings grown on LS agar media under LD or LD + FR + temp conditions were harvested at each time point, frozen in liquid nitrogen and stored at −80 °C. Total proteins were extracted using extraction buffer (50 mM sodium-phosphate pH 7.4, 100 mM NaCl, 10% glycerol, 5 mM EDTA, 1 mM dithiothreitol, 1% NP-40, 0.5% SDS, 0.5% sodium deoxycholate, 50 μM MG-132, 2 mM $NaVO_4$, 2 mM NaF and protease inhibitor tablets-EDTA free (Pierce)), and nuclei samples were prepared using the CelLytic Plant Nuclei Isolation/Extraction Kit (Sigma) based on the manufacturer's protocol.

To detect proteins, total protein extracts for phyA and ELF3, or nuclear extract for CO, were resolved in 9% or 11–12% SDS–PAGE gels, respectively, and transferred to nitrocellulose membranes (Bio-Rad). phyA, ELF3-6H3F and HA-CO proteins were detected using a monoclonal anti-phyA antibody[78] kindly provided by A. Nagatani (Kyoto University, Kyoto, Japan), anti-FLAG (A8592, Sigma) and anti-HA (3F10, Roche) antibodies. Actin or histone H3 proteins were used for internal loading controls of total protein or nuclear extract, respectively, and detected by anti-actin (C4, Millipore) and anti-histone H3 (ab1791, Abcam) antibodies, respectively.

For protein quantification, immunoreactive proteins on immunoblotted membranes were visualized with SuperSignal West Pico Luminol/Enhanced Solution (Thermo) and/or ECL Select Western Blotting Detection Reagent (Amersham) and imaged by ChemiDoc Touch (Bio-Rad). The image was used for quantification with the Image Lab program (Bio-Rad). Relative protein abundance was normalized against actin or histone H3.

Co-immunoprecipitation experiments. To analyse in vivo interactions, the *ELF3:ELF3-6H3F*, *35S:ELF3-6H3F*[44], *35S:3HA-CO* and *35S:3HA-CO 35S:ELF3-6H3F* lines grown under LD, LD + FR or LD + FR + temp conditions were harvested at ZT0, ZT2 or ZT4 on day 14, frozen in liquid nitrogen and stored at −80 °C. For analysing in planta interactions, the *35S:ELF3-6H3F*, *35S:3HA-CO*[46] and *35S:CO-TAP*[46] constructs were infiltrated into 3-week-old *Nicotiana benthamiana* leaves as previously described[46].

The method for co-immunoprecipitation assays was described previously[46]. Briefly, proteins were extracted from 1 ml volume of ground tissues using co-immunoprecipitation buffer (50 mM sodium-phosphate pH 7.4, 150 mM NaCl, 10% glycerol, 5 mM EDTA, 1 mM dithiothreitol, 0.1% Triton X-100, 50 μM MG-132, 2 mM $NaVO_4$, 2 mM NaF and protease inhibitor tablets-EDTA free (Pierce)) and incubated with Protein G-coupled magnetic beads (Dynabeads Protein G, Invitrogen) that captured anti-FLAG (F1804, Sigma) antibody at 4 °C for 10 min under dim light. After washing three times, precipitated proteins were eluted with 2× SDS sample buffer at 80 °C for 3 min. Fifty per cent of the eluted proteins and 1.5% of the total extract as an input were resolved in 9% SDS–PAGE gels. ELF-6H3F and endogenous phyA proteins were detected by western blot using anti-FLAG (Sigma) and anti-phyA antibodies, respectively.

Reporting Summary. Further information on research design is available in the Nature Research Reporting Summary linked to this article.

Data availability

All data are available in the main text or the Supplementary Materials. The raw sequence data (GSE110605) were deposited in the NCBI Sequence Read Archive.

The mass spectrometry proteomics data were deposited to the ProteomeXchange Consortium via the PRIDE partner repository with the data set identifier PXD010518 and 10.6019/PXD010518.

Received: 18 March 2018; Accepted: 16 August 2018;
Published online: 24 September 2018

References

1. Song, Y. H., Shim, J. S., Kinmonth-Schultz, H. A. & Imaizumi, T. Photoperiodic flowering: time measurement mechanisms in leaves. *Annu. Rev. Plant Biol.* **66**, 441–464 (2015).
2. Mouradov, A., Cremer, F. & Coupland, G. Control of flowering time: interacting pathways as a basis for diversity. *Plant Cell* **14**, S111–S130 (2002).
3. Song, Y. H., Ito, S. & Imaizumi, T. Flowering time regulation: photoperiod- and temperature-sensing in leaves. *Trends Plant Sci.* **18**, 575–583 (2013).
4. Golembeski, G. S. & Imaizumi, T. Photoperiodic regulation of florigen function in *Arabidopsis thaliana*. *Arabidopsis Book* **13**, e0178 (2015).
5. Blümel, M., Dally, N. & Jung, C. Flowering time regulation in crops—what did we learn from *Arabidopsis*? *Curr. Opin. Biotechnol.* **32**, 121–129 (2015).
6. Kubota, A. et al. Co-option of a photoperiodic growth-phase transition system during land plant evolution. *Nat. Commun.* **5**, 3668 (2014).
7. Mockler, T. et al. Regulation of photoperiodic flowering by *Arabidopsis* photoreceptors. *Proc. Natl Acad. Sci. USA* **100**, 2140–2145 (2003).
8. Ratcliffe D. *The Geographical and Ecological Distribution of* Arabidopsis *and Comments on Physiological Variation* (Arabidopsis Information Service, 1965); https://www.arabidopsis.org/ais/1965/ratcl-1965-aagli.html
9. Effmertova E. *The Behaviour of "Summer Annual", "Mixed", and "Winter Annual" Natural Populations as Compared with Early and Late Races in Field Conditions* (Arabidopsis Information Service, 1967); https://www.arabidopsis.org/ais/1967/effme-1967-aagph.html
10. Thompson, L. The spatiotemporal effects of nitrogen and litter on the population dynamics of *Arabidopsis thaliana*. *J. Ecol.* **82**, 63–68 (1994).
11. Donohue, K. Germination timing influences natural selection on life-history characters in *Arabidopsis thaliana*. *Ecology* **83**, 1006–1016 (2002).
12. Griffith, C., Kim, E. & Donohue, K. Life-history variation and adaptation in the historically mobile plant *Arabidopsis thaliana* (Brassicaceae) in North America. *Am. J. Bot.* **91**, 837–849 (2004).
13. Wilczek, A. M. et al. Effects of genetic perturbation on seasonal life history plasticity. *Science* **323**, 930–934 (2009).
14. Picó, F. X. Demographic fate of *Arabidopsis thaliana* cohorts of autumn- and spring-germinated plants along an altitudinal gradient. *J. Ecol.* **100**, 1009–1018 (2012).
15. Chiang, G. C. K. et al. Pleiotropy in the wild: the dormancy gene *DOG1* exerts cascading control on life cycles. *Evolution* **67**, 883–893 (2013).
16. Bieniawska, Z. et al. Disruption of the *Arabidopsis* circadian clock is responsible for extensive variation in the cold-responsive transcriptome. *Plant Physiol.* **147**, 263–279 (2008).
17. Imaizumi, T., Tran, H. G., Swartz, T. E., Briggs, W. R. & Kay, S. A. FKF1 is essential for photoperiodic-specific light signalling in *Arabidopsis*. *Nature* **426**, 302–306 (2003).
18. Imaizumi, T., Schultz, T. F., Harmon, F. G., Ho, L. A. & Kay, S. A. FKF1 F-box protein mediates cyclic degradation of a repressor of *CONSTANS* in *Arabidopsis*. *Science* **309**, 293–297 (2005).
19. Kinmonth-Schultz, H. A. et al. Cool night-time temperatures induce the expression of *CONSTANS* and *FLOWERING LOCUS T* to regulate flowering in *Arabidopsis*. *New Phytol.* **211**, 208–224 (2016).
20. Yamaguchi, A., Kobayashi, Y., Goto, K., Abe, M. & Araki, T. *TWIN SISTER OF FT* (*TSF*) acts as a floral pathway integrator redundantly with *FT*. *Plant Cell Physiol.* **46**, 1175–1189 (2005).
21. Krzymuski, M. et al. The dynamics of *FLOWERING LOCUS T* expression encodes long-day information. *Plant J.* **83**, 952–961 (2015).
22. Mizoguchi, T. et al. Distinct roles of *GIGANTEA* in promoting flowering and regulating circadian rhythms in *Arabidopsis*. *Plant Cell* **17**, 2255–2270 (2005).
23. Amasino, R. Seasonal and developmental timing of flowering. *Plant J.* **61**, 1001–1013 (2010).
24. Holmes, M. G. & Smith, H. The function of phytochrome in plants growing in the natural environment. *Nature* **254**, 512–514 (1975).
25. Wollenberg, A. C., Strasser, B., Cerdan, P. D. & Amasino, R. M. Acceleration of flowering during shade avoidance in *Arabidopsis* alters the balance between *FLOWERING LOCUS C*-mediated repression and photoperiodic induction of flowering. *Plant Physiol.* **148**, 1681–1694 (2008).
26. Kim, S. Y., Yu, X. & Michaels, S. D. Regulation of *CONSTANS* and *FLOWERING LOCUS T* expression in response to changing light quality. *Plant Physiol.* **148**, 269–279 (2008).
27. Bouché, F., Lobet, G., Tocquin, P. & Périlleux, C. FLOR-ID: an interactive database of flowering-time gene networks in *Arabidopsis thaliana*. *Nucleic Acids Res.* **44**, D1167–D1171 (2016).
28. Koornneef, M., Alonso-Blanco, C. & Vreugdenhil, D. Naturally occurring genetic variation in *Arabidopsis thaliana*. *Annu. Rev. Plant Biol.* **55**, 141–172 (2004).
29. Lee, J. H. et al. Regulation of temperature-responsive flowering by MADS-box transcription factor repressors. *Science* **342**, 628–632 (2013).
30. Pruneda-Paz, J. L. & Kay, S. A. An expanding universe of circadian networks in higher plants. *Trends Plant Sci.* **15**, 259–265 (2010).
31. Reed, J. W., Nagatani, A., Elich, T. D., Fagan, M. & Chory, J. Phytochrome A and phytochrome B have overlapping but distinct functions in *Arabidopsis* development. *Plant Physiol.* **104**, 1139–1149 (1994).
32. Johnson, E., Bradley, M., Harberd, N. P. & Whitelam, G. C. Photoresponses of light-grown *phyA* mutants of *Arabidopsis* (phytochrome A is required for the perception of daylength extensions). *Plant Physiol.* **105**, 141–149 (1994).
33. Genoud, T. et al. FHY1 mediates nuclear import of the light-activated phytochrome A photoreceptor. *PLoS Genet.* **4**, e1000143 (2008).
34. Mockler, T. C., Guo, H., Yang, H., Duong, H. & Lin, C. Antagonistic actions of *Arabidopsis* cryptochromes and phytochrome B in the regulation of floral induction. *Development* **126**, 2073–2082 (1999).
35. Valverde, F. et al. Photoreceptor regulation of CONSTANS protein in photoperiodic flowering. *Science* **303**, 1003–1006 (2004).
36. Reed, J. W. et al. Independent action of ELF3 and phyB to control hypocotyl elongation and flowering time. *Plant Physiol.* **122**, 1149–1160 (2000).
37. Leivar, P. & Quail, P. H. PIFs: pivotal components in a cellular signaling hub. *Trends Plant Sci.* **16**, 19–28 (2011).
38. Nusinow, D. A. et al. The ELF4–ELF3–LUX complex links the circadian clock to diurnal control of hypocotyl growth. *Nature* **475**, 398–402 (2011).
39. Jang, S. et al. *Arabidopsis* COP1 shapes the temporal pattern of CO accumulation conferring a photoperiodic flowering response. *EMBO J.* **27**, 1277–1288 (2008).
40. Laubinger, S. et al. *Arabidopsis* SPA proteins regulate photoperiodic flowering and interact with the floral inducer CONSTANS to regulate its stability. *Development* **133**, 3213–3222 (2006).
41. Nakamichi, N. et al. *Arabidopsis* clock-associated pseudo-response regulators PRR9, PRR7 and PRR5 coordinately and positively regulate flowering time through the canonical CONSTANS-dependent photoperiodic pathway. *Plant Cell Physiol.* **48**, 822–832 (2007).
42. Park, M. J., Kwon, Y. J., Gil, K. E. & Park, C. M. LATE ELONGATED HYPOCOTYL regulates photoperiodic flowering via the circadian clock in *Arabidopsis*. *BMC Plant Biol.* **16**, 114 (2016).
43. Lazaro, A., Valverde, F., Pineiro, M. & Jarillo, J. A. The *Arabidopsis* E3 ubiquitin ligase HOS1 negatively regulates CONSTANS abundance in the photoperiodic control of flowering. *Plant Cell* **24**, 982–999 (2012).
44. Huang, H. et al. Identification of evening complex associated proteins in *Arabidopsis* by affinity purification and mass spectrometry. *Mol. Cell. Proteomics* **15**, 201–217 (2016).
45. Schwartz, C. J., Lee, J. & Amasino, R. Variation in shade-induced flowering in *Arabidopsis thaliana* results from *FLOWERING LOCUS T* allelic variation. *PLoS ONE* **12**, e0187768 (2017).
46. Song, Y. H. et al. FKF1 conveys timing information for CONSTANS stabilization in photoperiodic flowering. *Science* **336**, 1045–1049 (2012).
47. Yu, J. W. et al. COP1 and ELF3 control circadian function and photoperiodic flowering by regulating GI stability. *Mol. Cell* **32**, 617–630 (2008).
48. Sheerin, D. J. et al. Light-activated phytochrome A and B interact with members of the SPA family to promote photomorphogenesis in *Arabidopsis* by reorganizing the COP1/SPA complex. *Plant Cell* **27**, 189–201 (2015).
49. Kim, W. Y., Hicks, K. A. & Somers, D. E. Independent roles for *EARLY FLOWERING 3* and *ZEITLUPE* in the control of circadian timing, hypocotyl length, and flowering time. *Plant Physiol.* **139**, 1557–1569 (2005).
50. Lin, M. K. et al. FLOWERING LOCUS T protein may act as the long-distance florigenic signal in the cucurbits. *Plant Cell* **19**, 1488–1506 (2007).
51. Yoo, S. C. et al. Phloem long-distance delivery of FLOWERING LOCUS T (FT) to the apex. *Plant J.* **75**, 456–468 (2013).
52. Mitchell, D. E., Gadus, M. V. & Madore, M. A. Patterns of assimilate production and translocation in muskmelon (*Cucumis melo* L.): I. Diurnal patterns. *Plant Physiol.* **99**, 959–965 (1992).
53. Savage, J. A., Zwieniecki, M. A. & Holbrook, N. M. Phloem transport velocity varies over time and among vascular bundles during early cucumber seedling development. *Plant Physiol.* **163**, 1409–1418 (2013).
54. Yasunaga, E., Yano, T., Araki, T., Setoyama, S. & Kitano, M. Effect of environmental condition on xylem and phloem transport of developing fruit. *IFAC Proc.* **46**, 297–301 (2013).
55. Shim, J. S., Kubota, A. & Imaizumi, T. Circadian clock and photoperiodic flowering in *Arabidopsis*: CONSTANS is a hub for signal integration. *Plant Physiol.* **173**, 5–15 (2017).
56. Pittendrigh, C. S. & Minis, D. H. The entrainment of circadian oscillations by light and their role as photoperiodic clocks. *Am. Nat.* **98**, 261–294 (1964).
57. Gattermann, R. et al. Golden hamsters are nocturnal in captivity but diurnal in nature. *Biol. Lett.* **4**, 253–255 (2008).

58. Daan, S. et al. Lab mice in the field: unorthodox daily activity and effects of a dysfunctional circadian clock allele. *J. Biol. Rhythms* **26**, 118–129 (2011).
59. Vanin, S. et al. Unexpected features of *Drosophila* circadian behavioural rhythms under natural conditions. *Nature* **484**, 371–375 (2012).
60. Montelli, S. et al. *period* and *timeless* mRNA splicing profiles under natural conditions in *Drosophila melanogaster*. *J. Biol. Rhythms* **30**, 217–227 (2015).
61. Shimizu, K. K., Kudoh, H. & Kobayashi, M. J. Plant sexual reproduction during climate change: gene function in natura studied by ecological and evolutionary systems biology. *Ann. Bot.* **108**, 777–787 (2011).
62. Kudoh, H. Molecular phenology in plants: in natura systems biology for the comprehensive understanding of seasonal responses under natural environments. *New Phytol.* **210**, 399–412 (2016).
63. Kotake, T., Takada, S., Nakahigashi, K., Ohto, M. & Goto, K. *Arabidopsis TERMINAL FLOWER 2* gene encodes a heterochromatin protein 1 homolog and represses both *FLOWERING LOCUS T* to regulate flowering time and several floral homeotic genes. *Plant Cell Physiol.* **44**, 555–564 (2003).
64. Takada, S. & Goto, K. TERMINAL FLOWER2, an *Arabidopsis* homolog of HETEROCHROMATIN PROTEIN1, counteracts the activation of F*LOWERING LOCUS T* by constans in the vascular tissues of leaves to regulate flowering time. *Plant Cell* **15**, 2856–2865 (2003).
65. Reed, J. W., Nagpal, P., Poole, D. S., Furuya, M. & Chory, J. Mutations in the gene for the red/far-red light receptor phytochrome B alter cell elongation and physiological responses throughout *Arabidopsis* development. *Plant Cell* **5**, 147–157 (1993).
66. Liu, X. L., Covington, M. F., Fankhauser, C., Chory, J. & Wagner, D. R. *ELF3* encodes a circadian clock-regulated nuclear protein that functions in an *Arabidopsis PHYB* signal transduction pathway. *Plant Cell* **13**, 1293–1304 (2001).
67. McNellis, T. W. et al. Genetic and molecular analysis of an allelic series of*cop1* mutants suggests functional roles for the multiple protein domains. *Plant Cell* **6**, 487–500 (1994).
68. Laubinger, S., Fittinghoff, K. & Hoecker, U. The SPA quartet: a family of WD-repeat proteins with a central role in suppression of photomorphogenesis in *Arabidopsis*. *Plant Cell* **16**, 2293–2306 (2004).
69. Leivar, P. et al. Multiple phytochrome-interacting bHLH transcription factors repress premature seedling photomorphogenesis in darkness. *Curr. Biol.* **18**, 1815–1823 (2008).
70. Yanovsky, M. J., Mazzella, M. A., Whitelam, G. C. & Casal, J. J. Resetting of the circadian clock by phytochromes and cryptochromes in *Arabidopsis*. *J. Biol. Rhythms* **16**, 523–530 (2001).
71. Yakir, E. et al. Posttranslational regulation of CIRCADIAN CLOCK ASSOCIATED1 in the circadian oscillator of *Arabidopsis*. *Plant Physiol.* **150**, 844–857 (2009).
72. Nakamichi, N., Kita, M., Ito, S., Yamashino, T. & Mizuno, T. PSEUDO-RESPONSE REGULATORS, PRR9, PRR7 and PRR5, together play essential roles close to the circadian clock of *Arabidopsis thaliana*. *Plant Cell Physiol.* **46**, 686–698 (2005).
73. Kubota, A. et al. TCP4-dependent induction of *CONSTANS* transcription requires GIGANTEA in photoperiodic flowering in *Arabidopsis*. *PLoS Genet.* **13**, e1006856 (2017).
74. Baudry, A. et al. F-box proteins FKF1 and LKP2 act in concert with ZEITLUPE to control *Arabidopsis* clock progression. *Plant Cell* **22**, 606–622 (2010).
75. Robinson, M. D., McCarthy, D. J. & Smyth, G. K. edgeR: a Bioconductor package for differential expression analysis of digital gene expression data. *Bioinformatics* **26**, 139–140 (2010).
76. Benjamini, Y. & Hochberg, Y. Controlling the false discovery rate: a practical and powerful approach to multiple testing. *J. R. Stat. Soc. Series B Stat. Methodol.* **57**, 289–300 (1995).
77. Huang da, W., Sherman, B. T. & Lempicki, R. A. Systematic and integrative analysis of large gene lists using DAVID bioinformatics resources. *Nat. Protoc.* **4**, 44–57 (2009).
78. Shinomura, T. et al. Action spectra for phytochrome A- and B-specific photoinduction of seed germination in *Arabidopsis thaliana*. *Proc. Natl Acad. Sci. USA* **93**, 8129–8133 (1996).
79. Jefferson, R. A., Kavanagh, T. A. & Bevan, M. W. GUS fusions: beta-glucuronidase as a sensitive and versatile gene fusion marker in higher plants. *EMBO J.* **6**, 3901–3907 (1987).

Acknowledgements

We thank M. Endo, M. Zeidler, X. W. Deng, U. Hoecker, R. Green, S. Harmer, T. Yamashino and J. H. Ahn for providing the mutant seeds, J. Nemhauser for critical reading of the manuscript and J. Milne for technical support. This work was supported by a NIH grant (GM079712) to T.I., NSF grants (IOS-1656076 to T.I. and IOS-1456796 to D.A.N.), Next-Generation BioGreen 21 Program (SSAC, PJ013386, Rural Development Administration, Republic of Korea) to Y.H.S. and T.I., BBSRC award (BB/N012348/1) to A.J.M., JST CREST grant (JPMJCR16O3), MEXT Kakenhi (18H04785) and Swiss National Science Foundation to K.K.S., and NRF grant (NRF-2015R1D1A1A01058948) to Y.H.S. We acknowledge a NSF grant (DBI-0922879) for LTQ-Velos Pro Orbitrap liquid chromatography–tandem mass spectrometry acquisition. A.K. is supported by the JSPS Postdoctoral Fellowships for Research Abroad.

Author contributions

T.I. conceived the project. Y.H.S., A.K. and T.I. designed the experiments. Y.H.S., A.K., M.S.K., M.F.C., N.L., E.R.T., D.L.C., D.Y.H., R.A., S.K.H., H.H., N.H.N., D.A.N., A.J.M. and T.I. performed the experiments and analyses. Y.H.S., A.K. and T.I. wrote the manuscript with the help of R.A., D.A.N., A.J.M. and K.K.S.

Competing interests

The authors declare no competing interests.

Additional information

Supplementary information is available for this paper at https://doi.org/10.1038/s41477-018-0253-3.

Reprints and permissions information is available at www.nature.com/reprints.

Correspondence and requests for materials should be addressed to Y.H.S. or T.I.

Publisher's note: Springer Nature remains neutral with regard to jurisdictional claims in published maps and institutional affiliations.

nature research

Corresponding author(s): Takato Imaizumi, Young Hun Song

Reporting Summary

Nature Research wishes to improve the reproducibility of the work that we publish. This form provides structure for consistency and transparency in reporting. For further information on Nature Research policies, see Authors & Referees and the Editorial Policy Checklist.

Statistical parameters

When statistical analyses are reported, confirm that the following items are present in the relevant location (e.g. figure legend, table legend, main text, or Methods section).

n/a	Confirmed	
☐	☒	The exact sample size (*n*) for each experimental group/condition, given as a discrete number and unit of measurement
☐	☒	An indication of whether measurements were taken from distinct samples or whether the same sample was measured repeatedly
☐	☒	The statistical test(s) used AND whether they are one- or two-sided *Only common tests should be described solely by name; describe more complex techniques in the Methods section.*
☐	☒	A description of all covariates tested
☐	☒	A description of any assumptions or corrections, such as tests of normality and adjustment for multiple comparisons
☐	☒	A full description of the statistics including central tendency (e.g. means) or other basic estimates (e.g. regression coefficient) AND variation (e.g. standard deviation) or associated estimates of uncertainty (e.g. confidence intervals)
☐	☒	For null hypothesis testing, the test statistic (e.g. *F*, *t*, *r*) with confidence intervals, effect sizes, degrees of freedom and *P* value noted *Give P values as exact values whenever suitable.*
☒	☐	For Bayesian analysis, information on the choice of priors and Markov chain Monte Carlo settings
☒	☐	For hierarchical and complex designs, identification of the appropriate level for tests and full reporting of outcomes
☒	☐	Estimates of effect sizes (e.g. Cohen's *d*, Pearson's *r*), indicating how they were calculated
☐	☒	Clearly defined error bars *State explicitly what error bars represent (e.g. SD, SE, CI)*

Our web collection on statistics for biologists may be useful.

Software and code

Policy information about availability of computer code

Data collection	For gene expression analysis, CFX Manager Software (ver 3.1, #1845000, BioRad), followed by Microsoft Excel (Microsoft Office Professional Plus 2016, ver 16.0.6568.2025) was used.
Data analysis	Statistical analysis for flowering time experiments was done using R Statistical Computing software (v3.2.3; R Core Team, 2015). In RNA-seq analysis, Python library(clipper.py, https://github.com/mfcovington/clipper), followed by Perl script (simple_counts.pl, https://github.com/mfcovington/read_counter) was used to process the sequence files and read counts. The R package edgeR was used to identify differentially expressed genes across tested conditions. In TAP-IP analysis, ProteomeDiscoverer (ThermoFisherScientific; v.1.4) was used to extract the peaks and generate the mgf files which were submitted to Mascot (MatrixScience,London,UK;v.2.5.0) for database search (Huang et al., 2016 doi: 10.1016/j.dib.2016.05.014).

For manuscripts utilizing custom algorithms or software that are central to the research but not yet described in published literature, software must be made available to editors/reviewers upon request. We strongly encourage code deposition in a community repository (e.g. GitHub). See the Nature Research guidelines for submitting code & software for further information.

Data

Policy information about availability of data

All manuscripts must include a data availability statement. This statement should provide the following information, where applicable:

- Accession codes, unique identifiers, or web links for publicly available datasets
- A list of figures that have associated raw data
- A description of any restrictions on data availability

There is no restriction on material or data availabilities. All the materials were described in the main text or supplementary materials. The raw sequence data (GSE110605) were deposited in the NCBI Sequence Read Archive.

Field-specific reporting

Please select the best fit for your research. If you are not sure, read the appropriate sections before making your selection.

☒ Life sciences ☐ Behavioural & social sciences

For a reference copy of the document with all sections, see nature.com/authors/policies/ReportingSummary-flat.pdf

Life sciences

Study design

All studies must disclose on these points even when the disclosure is negative.

Sample size	Sample size was chosen based on previous studies and experience (no statistical methods were used previously to predetermine the sample sizes). For the gene expression and protein analysis, a minimum number of three independent biological replicates were used. Each sample consists of multiple individuals (<10). For flowering time measurement, a minimum of one independent biological replicate, which contained at least eleven individual plants, was used to analyze the phenotype.
Data exclusions	No data was excluded from this submission.
Replication	For flowering experiments in field conditions in Seattle, we confirmed reproducibility for at least 2 years. A similar tendency was observed in different locations of similar latitudes (in Edinburgh and Zurich), independently. For experiments performed under controlled laboratory conditions, data reproducibility was confirmed by independent biological trials performed by different authors.
Randomization	We did not apply randomization. In order to avoid a positional effect in our growth chambers or under field conditions, the positions of each plant were randomly circulated.
Blinding	We did not apply blinding. However, during the repetitive experiments performed by different authors, similar results were obtained.

Materials & experimental systems

Policy information about availability of materials

n/a	Involved in the study
☐	☒ Unique materials
☐	☒ Antibodies
☒	☐ Eukaryotic cell lines
☒	☐ Research animals
☒	☐ Human research participants

Unique materials

Obtaining unique materials	All materials used in this study are commonly available.

Antibodies

Antibodies used	Anti-phyA antibody was provided by Dr. Akira Nagatani (Simomura et al., PMIDI:8755615). Anti-FLAG (A8592, Sigma), and anti-HA (3F10, Roche) antibodies, anti-actin (C4, Millipore), anti-histone H3 (ab1791, Abcam) were used as primary antibodies. Goat anti-rabbit IgG (31460, Thermo Fisher Scientific), and anti-mouse IgG (31430, Thermo Fisher Scientific) were used as secondary antibodies. The dilution rates are 1:2,000 for anti-phyA, 1:5,000 for anti-FLAG, 1:1,000 for anti-HA, 1:5,000 for anti-Actin, 1:10,000 for anti-Histone H3, 1:20,000 for anti-Rabbit IgG and 1:20,000 for anti-Mouse IgG.
Validation	Anti-phyA specificity was confirmed by previous studies (Simomura et al., PMIDI:8755615). Anti-HA or anti-FLAG specificities against tagged-CO protein is described in Song et al., 2012 (doi:10.1126/science.1219644PMID), Song et al., 2016 (doi: 10.1073/pnas.1415375111). Anti-flag specificity against tagged-ELF3 protein is described in Huang et al., 2016 (doi: 10.1074/

mcp.M115.054064). In addition, we confirmed the specificity of each protein of interest by loading WT plants or mutant plants as negative controls together with the samples to be tested.

Method-specific reporting

n/a	Involved in the study
☒	☐ ChIP-seq
☒	☐ Flow cytometry
☒	☐ Magnetic resonance imaging